Bull. Mater. Sci. (2018) 41:35
https://doi.org/10.1007/s12034-018-1553-y

Fe_2O_3/MWCNTs nanocomposite decorated glassy carbon electrode for the determination of nitrite

XIU RU LIN[1,2], YI FAN ZHENG[3] and XU CHUN SONG[1,*]

[1]Department of Chemistry, Fujian Normal University, Fuzhou 350007, People's Republic of China
[2]Fujian Provincial Key Laboratory of Featured Materials in Biochemical Industry, Ningde Normal University, Ningde 352100, People's Republic of China
[3]Research Center of Analysis and Measurement, Zhejiang University of Technology, Hangzhou 310014, People's Republic of China
*Author for correspondence (songxuchunfj@163.com)

MS received 3 May 2017; accepted 1 July 2017; published online 23 March 2018

Abstract. A novel ferric oxide/multi-walled carbon nanotubes (Fe_2O_3/MWCNTs)-modified glassy carbon electrode (GCE) was prepared by drop casting Fe_2O_3/MWCNTs onto the surface of GCE. Scanning electron microscopy (SEM) image shows that the Fe_2O_3/MWCNTs has a nanostructure. Cyclic voltammetry (CV) results show that the Fe_2O_3/MWCNTs-modified GCE presents excellent electrochemical activity in the presence of 1 mM nitrite in a 0.1 M phosphate-buffered saline (PBS) to compare the Fe_2O_3 and MWCNTs-modified GCE. Differential pulse voltammetry (DPV) results also show that the Fe_2O_3/MWCNTs has excellent electrocatalytic performance to nitrite in a pH 7.0 PBS. The amperometric response result shows that the Fe_2O_3/MWCNTs-modified GCE can be used to detect nitrite concentration in a wide linear range of 10–1000 μM with a detection limit of 0.1 μM.

Keyword. Fe_2O_3; MWCNTs; electrochemical determination; nitrite.

1. Introduction

As is known to all that nitrite is universally found within the live process and environment and is generally used as a corrosion inhibitor or additive in some foods [1,2]. However, carcinogenic nitrosamines can be formed by nitrite when interact with amines [3]. Therefore, it is critical and necessary to carry out the detection of nitrite in practical analysis. In recent years, many methods were developed for the determination of nitrite [4]. Among them, electrochemical techniques were widely adopted because of their properties with simple use and rapid response [5]. Generally, the electrochemical analysis of the nitrite can be completed based on the electrochemical reduction or oxidation of nitrite. However, it should be indicated that the reduction potential is extremely negative for nitrite, and it is difficult to use its reduction behaviour to detect nitrite directly. Therefore, many catalysts are used to promote the electroreduction of nitrite [6]. Recently, Zhao *et al* [7] prepared the sensor based on palladium-nanoparticle-functionalized multi-walled carbon nanotubes (MWCNTs) for electrochemical detection of the oxidation of NO_2. Liu *et al* [8] reported nitrogen and phosphorus co-doped graphene quantum dots for electroanalysis of NO_2. Though their work showed high sensitivity, however, their work also showed some disadvantages, such as high cost and complicated material preparation process. Therefore, the electrochemical detection of nitrite with high selectivity and sensitivity is still challenging, although the electro-catalysis of nitrite was enhanced greatly. Recently, more efforts are being made to improve the selectivity and sensitivity.

At present, the electrochemical sensor preparation from nanocomposites-modified electrodes was recognized increasingly. Recently, iron oxide nanomaterials have attracted tremendous attention in the areas of electrochemical sensors and nanotechnology, because of their excellent catalytic properties and interesting electron transport behaviour [9–13]. Hematite (α-Fe_2O_3), maghemite (γ-Fe_2O_3) and magnetite (Fe_3O_4) are probably the most general oxides of many oxide modalities in which oxides of iron exist in nature. In particular, α-Fe_2O_3 nanomaterials were of technological and scientific interest due to their biocompatibility, low toxicity and magnetic properties in physiological environments. It is used in many fields, such as magnetically assisted drug delivery, magnetic resonance imaging (MRI), information storage, wave adsorption and anode material [14]. Recently, Fe_2O_3 was tentatively found as a potential activity and explored as an electrocatalyst towards hydrogen peroxide, glucose and reduced nicotinamide cofactors.

Carbon nanotubes have drawn more attention due to their high mechanical strength, excellent electrical conductivity, high surface area and chemical stability [15]. Recently, nanocomposites containing polythionine CNTs [16], carbon nanotubes–ionic liquids [17], CNTs–cobalt nanoparticles [18], catalase–CNTs [19], CNTs ionic liquids–Pt–Au alloy

nanoparticles [20], vanadium shiefbase–CNTs [21], CNTs–iron porphyrin [22], silica–cerium mixed oxide carbon paste [23] and CNTs–poly thiophene [24] were used for the electrochemical detection of nitrite. Although all these chemical sensors are favourable for nitrite detection, some of them give relatively poor selectivity and repeatability, low sensitivity and reproducibility with short-time stability under complicated multi-step preparation methods and physiological condition. In addition, the electrocatalytic behaviour of the modified electrode was restricted only for oxidation or reduction of the nitrite. Wang *et al* [25] reported an efficient method of using Pt nanoparticles to decorate CNx nanotubes. It is mentioned in the report that using metal/metal oxide to decorate CNT surfaces effectively improves the emission-site density, and the work is of great importance for future electronic display devices.

In this work, we report a facile composition of MWCNTs/Fe_2O_3 nanocomposites, and its application to the electrochemical detection of nitrite. Electrochemical studies showed that the composite exhibited a low detection limit and a wide linear range to nitrite with a fast current response. In addition, the modified electrode showed long-term stability and excellent reproducibility. The fabricated electrochemical sensor displayed significant selectivity, sensitivity and it was also used to real sample analysis.

2. Experimental

2.1 *Materials*

MWCNTs, potassium ferricyanide ($K_3[Fe(CN)_6]$), sodium nitrite ($NaNO_2$), 0.1 mol l^{-1} phosphate buffer solution (PBS) is made up of disodium hydrogen phosphate (Na_2HPO_4) and two hydrated sodium dihydrogen phosphate ($NaH_2PO_4 \cdot 2H_2O$), hydrochloric acid (HCl), sodium hydroxide (NaOH) and dimethyl formamide (DMF). All other reagents were of analytical grade and were used as received without further treatment.

2.2 *Apparatus*

Electrochemical experiment technology including chronoamperometry (CA), differential pulse voltammetry (DPV) and cyclic voltammetry (CV) were carried out on CHI660 electrochemical work station (Chenhua, Shanghai, China) with traditional three-electrode system, among them, the platinum electrode as the counter electrode, Ag/AgCl ((sat) KCl) electrode as the reference electrode, and glassy carbon electrode (GCE) and its modified electrode as working electrodes. The morphologies and structures of samples were carried out by a Hitachi S-4700 SEM (scanning voltages was 15 kV). Powder X-ray diffraction (XRD) was performed using a Thermo ARL SCINTAG X'TRA X-ray diffractometer with CuKα radiation ($\lambda = 0.154056$ nm) in the 2θ range of 20–70°.

2.3 *Synthesis of Fe_2O_3 /MWCNTs nanocomposite*

Fe_2O_3 was synthesized through a hydrothermal method, which was reported previously [26]. In a typical preparation of Fe_2O_3/MWCNTs, 197.6 mg $K_3[Fe(CN)_6]$ was dissolved in 40 ml of distilled water with pH of 12, and then, 60.0 mg of the MWCNTs were added into the solution. Next, the homogeneous solution was poured into a 50 ml Teflon-lined autoclave and held at 160°C for 24 h. Then, the reddish brown precipitate was collected by centrifugation, which was washed three times with ethanol and distilled water, and then dried in the oven at 60°C for 12 h. As a control experiment, Fe_2O_3 nanometre material was prepared without adding MWCNTs under the same conditions.

2.4 *Preparation of the modified electrode*

Prior to modification, a 3 mm diameter GCE was polished with alumina slurry of 3 and 0.5 μM on polishing cloth with water, respectively, and then thoroughly rinsed with anhydrous ethanol and sonicated in ultrapure water bath for 5 min before use. For preparation of the electrochemical sensor, 5 mg samples and 5 ml dimethyl formamide (DMF) were dispersed by ultrasonication for 25 min to gain a homogeneous suspension (1.0 mg ml^{-1}). Then, 5 μl of the suspension was dropped onto the surface of GCE and was dried at room temperature.

3. Results and discussion

Figure 1a represents SEM pattern of the Fe_2O_3/MWCNTs nanocomposite. SEM image of the composite displayed almost uniform sized Fe_2O_3 nanoparticles, which were dispersed on the MWCNTs surface. The successful synthesis of Fe_2O_3/MWCNTs nanocomposites was further confirmed. Figure 1b shows the transmission electron microscopy (TEM) images of Fe_2O_3/MWCNTs nanocomposite. The TEM images show that the Fe_2O_3 nanoparticles are doped with MWCNTs. In addition, a high-resolution TEM (HRTEM) image of Fe_2O_3/MWCNTs nanocomposite is shown in figure 1c. The clear lattice fringes ($d = 0.344$ nm) observed in the HRTEM image agree well with the (002) lattice planes of MWCNTs, and the lattice fringes of (104) planes ($d = 0.271$ nm) are assigned to Fe_2O_3. Figure 1d illustrates the elemental composition of the electrode surface. The energy dispersive X-ray analysis (EDX) spectrum confirms the existence of C, Fe and O on the electrode surface. Figure 2 illustrates the XRD image of the Fe_2O_3/MWCNTs nanocomposite. The MWCNTs exhibited one significant diffraction peak at $2\theta = 26$, attributed to the (0 0 2) reflections of carbon nanotubes. In addition, the nanocomposite exhibited nine obvious diffraction peaks, and which were indexed to the (0 1 2), (1 0 4), (1 1 0), (1 1 3), (0 2 4), (1 1 6), (0 1 8), (2 1 4) and (3 0 0) planes of the pure Fe_2O_3. The narrow and sharp peaks indicate that these Fe_2O_3/MWCNTs nanocomposite are

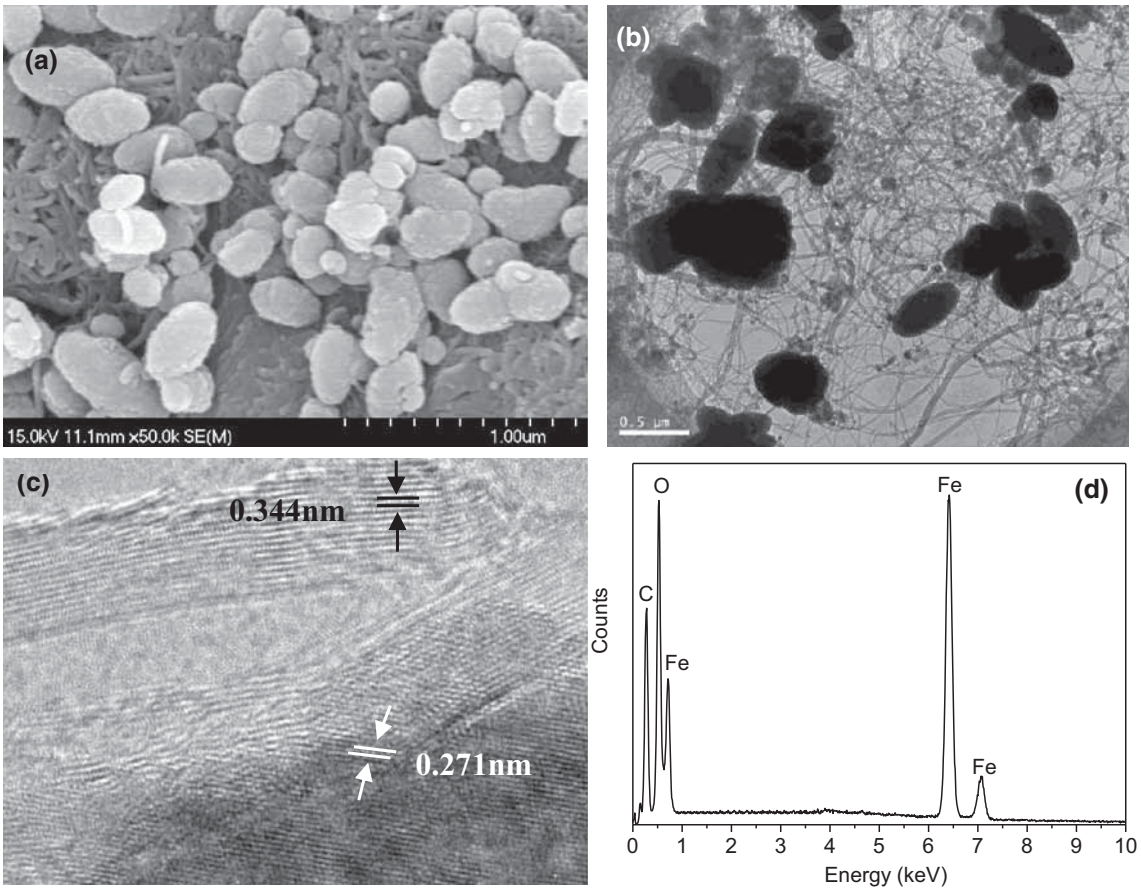

Figure 1. (**a**) SEM, (**b**) TEM, (**c**) HRTEM and (**d**) EDX patterns of the Fe_2O_3/MWCNTs nanocomposite.

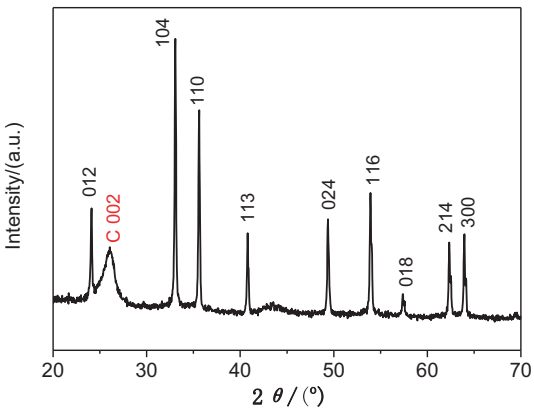

Figure 2. XRD pattern of the Fe_2O_3/MWCNTs. nanocomposite.

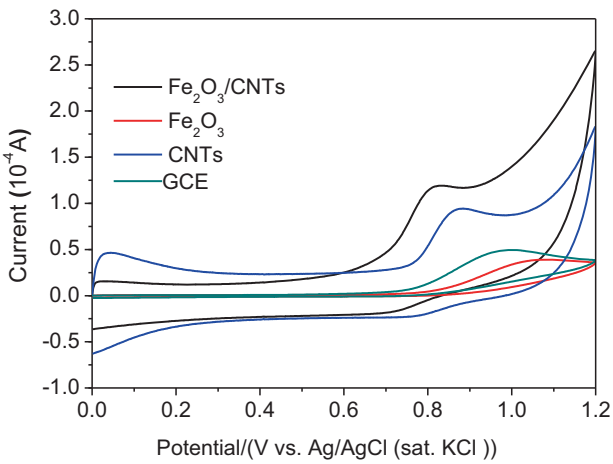

Figure 3. CVs of bare GC electrode, Fe_2O_3, MWCNTs and Fe_2O_3/MWCNTs-modified GCE in the presence of 1 mM nitrite in a 0.1 M PBS (pH 7.0) at a scan rate of 100 mV s^{-1}.

well-crystallized. These results proved the existence of both MWCNTs and Fe_2O_3 in the as-synthesized composite.

Figure 3 shows the CVs of the bare GCE, Fe_2O_3/GCE, MWCNTs/GCE and Fe_2O_3/MWCNTs/GCE in the presence of 1 mM nitrite in a 0.1 M PBS (pH 7.0) at a scan rate of 100 mV s^{-1}. The anodic peak current of the MWCNTs/GCE is greater than that of the bare GCE, which can be attributed to that the large specific surface area of MWCNTs. The background current of the Fe_2O_3/MWCNTs/GCE was much larger than the Fe_2O_3/GCE and bare GCE, which may be due to the synergy of ferric oxide and carbon

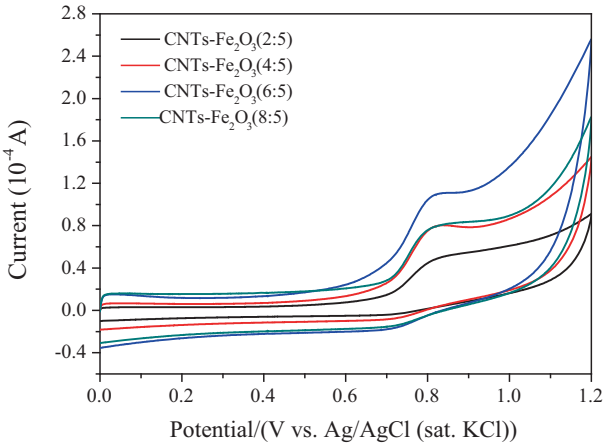

Figure 4. Different mass ratio of Fe_2O_3/MWCNTs cyclic voltammograms in the presence of 1 mM nitrite in a 0.1 M PBS (pH 7.0) at a scan rate of 100 mV s^{-1}.

nanotubes. Different mass ratio of composites make different electrochemical behaviours of nitrite detection. To explore the best proportion, we created different mass ratios of composite materials towards nitrite detection through CV. CVs (figure 4) were recorded to understand the electrochemical behaviour of Fe_2O_3/MWCNTs composites with different proportions modified electrode in a 0.1 M PBS solution in the presence of nitrite. It can be seen, when the mass ratio for 5:6 than catalytic peak is the largest, which may be at the time of the proportion, the synergy is of best. Hence, the electrode material was made according to the optimal proportion.

Figure 5a presents the CVs of the Fe_2O_3/MWCNTs/GCE in pH 7.0 PBS containing 1.0 mM nitrite at different scan rates. From this figure, we can see a positive shift in the peak potential and an augment in the anodic peak current as scan rate increases. The positive change of potential may be attributed to the dynamic control of the redox reaction between the Fe_2O_3/MWCNTs and the nitrite. This reaction is irreversible, and the E_{pa} obeys the Laviron's equation. Figure 5b shows that the catalytic peak of nitrite is proportional to the square root of scan rate (υ) in the range of 20–260 mV s^{-1}, and the linear equation can be exhibited by I_{pa} (mA) $= 10.08948 + 2.8075\upsilon^{1/2}$ with $R = 0.99211$. These results demonstrated that the electrocatalytic oxidation behaviour of nitrite was a diffusion-controlled process.

In general, the type of the solution, pH value and supporting electrolyte are essential factors to the electrochemical reaction. In comparison with the reaction of nitrite in B–R buffer solution and acetum buffer solution, a more sensitive catalytic peak of NO_2^- with more desirable peak shape was acquired in PBS buffer solution (results not shown). Therefore, PBS was chosen for the investigation of this experiment [7]. The effect of buffer solution pH value on the electrochemical response of 1.0 mM NO_2^- was explored in the range of 3.0–9.0 in PBS. As shown in figure 6, the anodic peak current of NO_2^- was influenced by pH value greatly. When pH was <7.0, with the

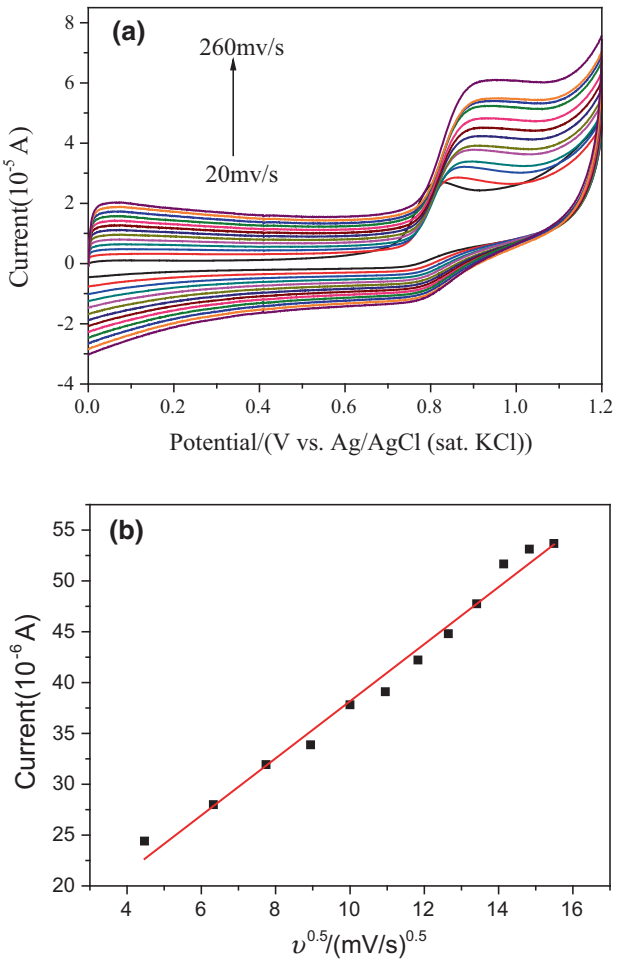

Figure 5. (**a**) CVs of the Fe_2O_3/MWCNTs/GCE at different scan rates (20–260 mV s^{-1}) in the presence of 1 mM nitrite and (**b**) the catalytic current value versus square root of the scan rate.

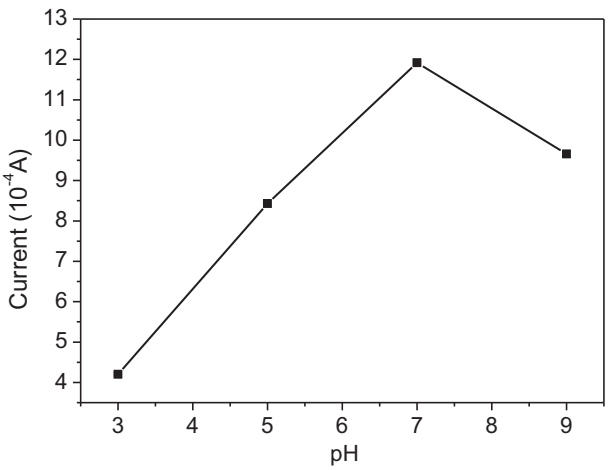

Figure 6. Buffer solution pH effects on $NaNO_2$ current response using Fe_2O_3/MWCNTs/GCE.

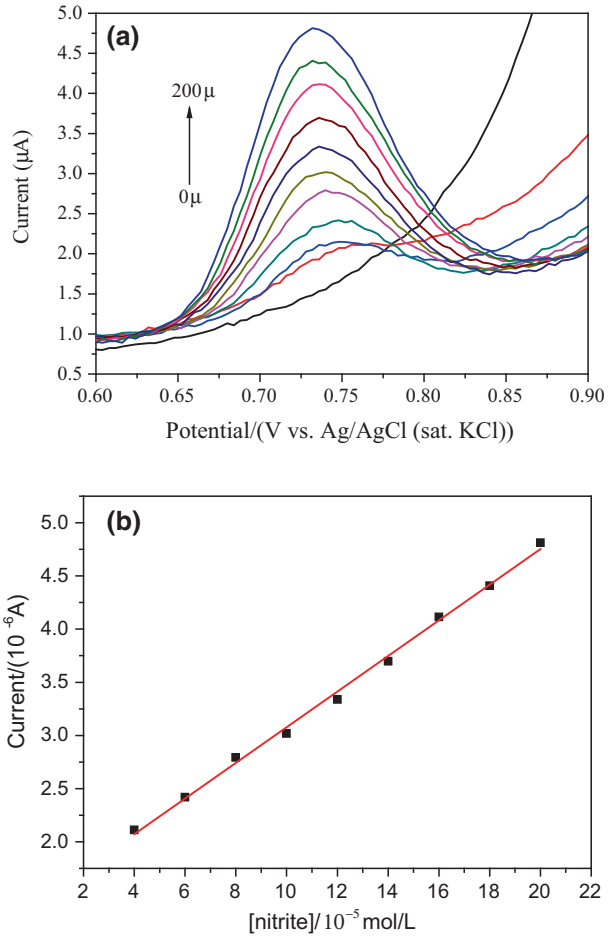

Figure 7. (**a**) DPVs of $NaNO_2$ at Fe_2O_3/MWCNTs/GCE in pH 7.0 PBS. $NaNO_2$ concentrations: 0, 20, 40, 60, 80, 100, 120, 140, 160, 180 and 200 μM. (**b**) Linear relationship between peak current and the concentration of $NaNO_2$.

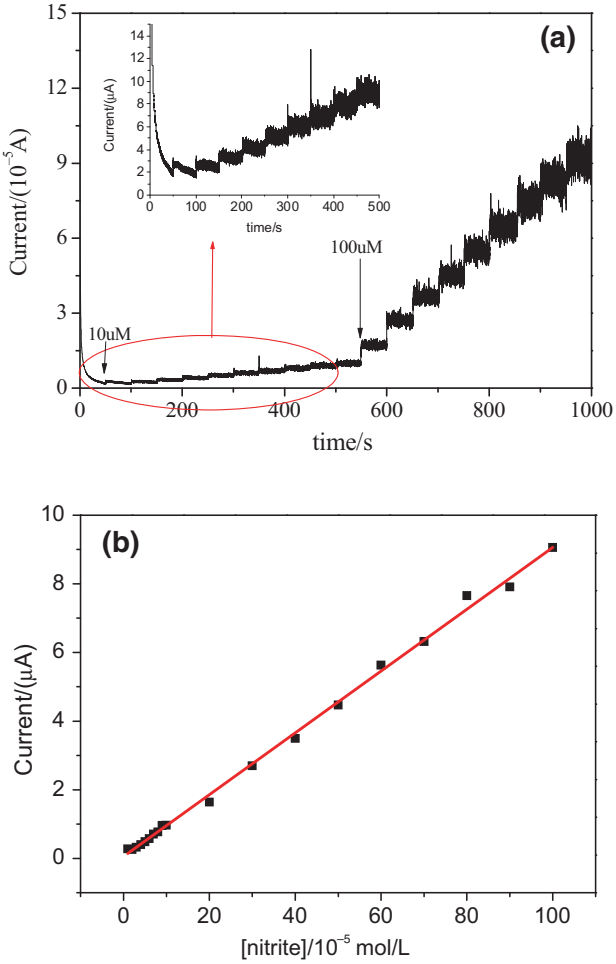

Figure 8. (**a**) Amperometric response curves of Fe_2O_3/MWCNTs/GCE upon successive addition of nitrite at 0.85 V. Inset: the amperometric response of low concentration of nitrite. (**b**) The relationship between nitrite concentration and current signal.

decrease in pH the catalytic peak decreased. To the best of our knowledge, in strong acidic medium, nitrites were not stable and could undergo the following conversion:

$$2H^+ + 3NO_2^- \rightarrow 2NO + NO_3^- + H_2O.$$

The decrease in anodic peak current at lower pH value (<7.0) may be attributed to the transformation of nitrite to nitric oxide and nitrate [27,28]. On the other hand, due to the pKa of nitrous acid, which was 3.3, most NO_2^- was protonated in acidic solution. Protonation was proved to refer to the catalytic oxidation process, and the active substance should be nitrous acid instead of nitrite [29–32]. When pH was >7.0, the electrocatalytic oxidation of NO_2^- became more difficult, and may be attributed to the shortage of proton [33–36]. Hence, with the increase in buffer solution pH, the catalytic peak decreased. The maximal anodic peak current was obtained at pH 7.0, which was employed as the optimum pH in our experiments.

Under the optimum conditions, the catalytic peak of different nitrite concentrations at the Fe_2O_3/MWCNTs/GCE were recorded by DPV in static solutions. As shown in figure 7a, the anodic peak current was proportional to the concentration of NO_2^- in the range of 2.0×10^{-5} to 2.0×10^{-4} M. The linear relationship between peak current and the concentration of $NaNO_2$ was showed in figure 7b. The linear regression equation can be expressed by $I_{pa}(\mu A) = 0.1674\,C(10^{-5}M) + 1.4023(n = 10, R = 0.9992)$, and showed a low detection limit of 2.0×10^{-7} M (S/N = 3).

Figure 8a presents the amperometric response of the Fe_2O_3/MWCNTs/GCE to successive additions of nitrite in 0.1 M PBS. An obvious increase in anodic peak current was obtained when nitrite was drip into the stirred PBS. The Fe_2O_3/MWCNTs/GCE electrode responded rapidly to the NO_2^-, reaching a plateau within 4 s. Figure 8b shows the relationship between the peak current of the Fe_2O_3/MWCNTs/GCE and the concentration of nitrite. The catalytic peak at

Table 1. Comparison of Fe_2O_3/ MWCNTs/GCE with other sensors for nitrite detection.

Electrode	Response range	LOD	Ref.
α-Fe_2O_3 NAs/CF	0.5–1000 μM	0.12 μM	[37]
Co_3O_4/RGO	1–380 μM	0.14 μM	[38]
Zr-MOF	20–800	2.1	[39]
Au/Zn-MOF	5–65,000 μM	0.4 μM	[40]
Au/ZnO/MWCNT	0.78–400 μM	2 μM	[6]
Pd/graphite	0.3–50.7 μM	0.071 μM	[41]
Fe_2O_3/MWCNTs	10–1000 μM	0.1 μM	This study

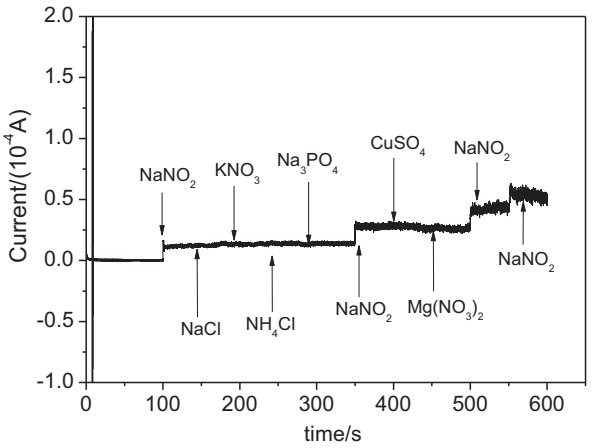

Figure 9. Amperometric response of modified electrode for 100 μM nitrite and different interferences, pH 7 and applied potential was 0.8 V.

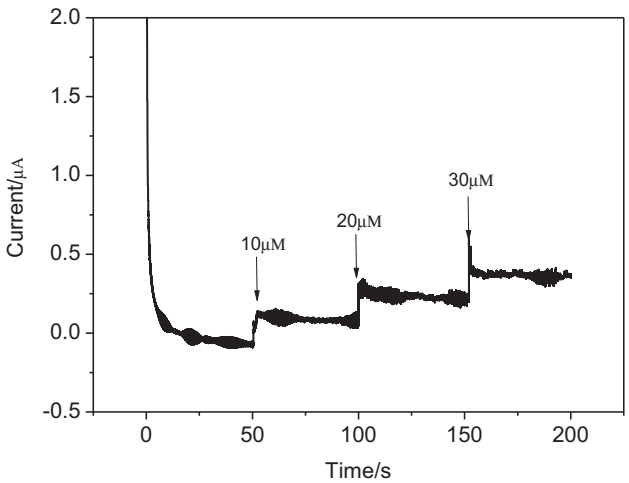

Figure 10. Amperometric response of modified electrode upon successive addition of 10, 20 and 30 μM nitrite spiked samples in tap water.

the Fe_2O_3/MWCNTs/GCE are proportional to the various concentrations of NO_2^- in the range of 10–1000 μM. The linear regression equation can be expressed by $I_{pa}(\mu A) = 0.9013C\,(10^{-5}M) + 0.52571(R = 0.9988)$. The limit of detection was 0.1 μM, which is about three order of the magnitude lower than the tap water limit quantity postulated by the WHO (43 μM). To evaluate the activity of the proposed nitrite sensor, other nitrite modified electrodes were listed in table 1 for comparison. Clearly, this nitrite sensor exhibits a comparable activity to others reported previously. Therefore, the Fe_2O_3/MWCNTs/GCE can be used for the preparation of a nitrite sensor with a low limit, and a wide linear range.

Selectivity is an significant parameter of the nitrite electrochemical sensor. Various common ions, such as Mg^{2+}, NH_4^+, Na^+, PO_4^{3+}, SO_4^{2-}, NO_3^- and Cl^-, did not interfere with the determination of nitrite. Figure 9 showed that no significant response currents were observed when 0.1 mM each of NaCl, KNO_3, NH_4Cl, Na_3PO_4, $CuSO_4$ and $Mg(NO_3)_2$ were injected at regular intervals. However, upon the addition of 0.1mM nitrite, a significant amperometric response was immediately observed, demonstrating the excellent selectivity of the Fe_2O_3/MWCNTs/GCE towards nitrite determination.

For real sample analysis, the preparative Fe_2O_3/MWCNTs/GCE sensor was used to detect nitrite levels in tap water. Tap water samples consisting of various concentrations of spiked NO_2^- were quantitatively analysed through a standard addition method. Before analysis, the samples were filtered by using a 0.2 μm filter to eliminate micron-sized particles. Figure 10 is the amperometric response curve of modified electrode upon successive addition of the 10, 20 and 30 μM nitrite spiked samples in tap water at 0.85 V. The results exhibited that the sensor was highly sensitive and selective to nitrite. The recoveries (table 2) were observed as 97.8, 99.5 and 101.2% for the 10, 20 and 30 μM nitrite spiked samples, respectively. These results indicated that the Fe_2O_3/MWCNTs/GCE modified electrode showed excellent determination of nitrites in tap water.

4. Conclusion

In summary, it is the first time that an unprecedented nitrite sensor based on tron oxide/carbon nanotube composite materials (Fe_2O_3/MWCNTs/GCE) was developed. The Fe_2O_3/MWCNTs/GCE-modified electrode has excellent catalytic efficiency and highly electron transfer rate constant towards the catalytic oxidation of nitrite compared to undecorated electrode. CV, DPV and CA were used to verify the

Table 2. Determination of nitrite in tap water using Fe_2O_3/MWCNTs/GCE.

Samples	Added (μM)	Found (μM)	Recovery (%)	RSD (%)
Sample 1	10.0	9.78	97.8	3.7
Sample 2	20.0	19.91	99.5	4.4
Sample 3	30.0	30.36	101.2	2.9

electrocatalytic performance of the proposed sensor. The dynamic linear range and obtained limit of detection indicate that the sensor exhibited low detection limit and a wide linear range. The modified electrodes for various interferences such as of NaCl, KNO_3, NH_4Cl and other important cations and anions is negligible. Based on this experiment it is anticipated that proposed sensor could be used to the detection of nitrite in real sample such as tap water successfully. Fe_2O_3/MWCNTs/GCE-modified electrode can be applied as a promising candidate for determination of nitrite sensor or detector, because of its high simplicity, sensitivity, reproducibility and selectivity, low detection limit, rapid analysis procedure and long-term stability.

References

[1] Zhao K, Song H Y, Zhuang S Q, Dai L M, He P G and Fang Y Z 2007 *Electrochem. Commun.* **9** 65

[2] Alonso A, Etxaniz B and Martinez M D 1992 *Food Addit. Contam.* **9** 111

[3] Bruning-Fann C S and Kaneene J B 1993 *Vet. Hum. Toxicol.* **35** 521

[4] Kamyabi M A and Aghajanloo F 2008 *J. Electroanal. Chem.* **614** 157

[5] Wen Z H and Kang T F 2004 *Talanta* **62** 351

[6] Lin A J, Wen Y, Zhang L J, Lu B, Li Y, Jiao Y Z *et al* 2011 *Electrochim. Acta* **56** 1030

[7] Thirumalraj B, Palanisamy S, Chen S M and Zhao D H 2016 *J. Colloid Interface Sci.* **478** 413

[8] Liu R G, Zhao J J, Huang Z R, Zhang L L, Zou M B, Shi B F *et al* 2017 *Sens. Actuators B* **240** 604

[9] Mimica D, Zagal J H and Bedioui F 2001 *J. Electroanal. Chem.* **497** 106

[10] Adekunle A S and Ozoemena K I 2010 *J. Electrochem. Sci.* **5** 1726

[11] Zhang Y P, Chu Y and Dong L H 2007 *Nanotechnology* **18** 435608

[12] Neri G, Bonavita A, Galvagno S, Siciliano P and Capone S 2002 *Sens. Actuators B* **82** 40

[13] Mitra S, Das S, Mandal K and Chuadhari S 2007 *Nanotechnology* **18** 275608

[14] He Y, Zeng K, Zhang X, Gurung A, Baloda M, Xu H *et al* 2010 *Electrochem. Commun.* **12** 985

[15] Mou F Z, Guan J G, Xiao Z D, Sun Z G, Shi W D and Fan X A 2011 *J. Mater. Chem.* **21** 5414

[16] Yonezawa T, Onoue S and Kimizuka N 2001 *Adv. Mater.* **13** 140

[17] Deng C, Chen J, Nie Z, Yang M and Si S 2012 *Thin Solid Films* **520** 7026

[18] Xiao F, Li L, Li J, Zeng J and Zeng B 2008 *Electroanalysis* **20** 2047

[19] Adekunle A S, Pillay J and Ozoemena K I 2010 *Electrochim. Acta* **55** 4319

[20] Salimi A, Mamkhezri H and Mohhebbi S 2006 *Electrochem. Commun.* **8** 688

[21] Xiao F, Mo Z, Zhao F and Zeng B 2008 *Electrochem. Commun.* **10** 1740

[22] Salimi A, Noorbakhsh A and Ghadermazi M 2007 *Sens. Actuators B* **123** 530

[23] Turdean G L, Popescu I C, Curulli A and Palleschi G 2006 *Electrochim. Acta* **51** 6435

[24] Morais A D, Villis P C M, Maroneze C M, Gushikem Y, Lucho A M S and Pissetti F L 2012 *J. Colloid Interface Sci.* **369** 302

[25] Ghosh K, Kumar M, Wang H F, Maruyama T and Ando Y 2010 *J. Phys. Chem. C* **114** 5107

[26] Lin C Y, Vasantha S V and Ho K C 2010 *Sens. Actuators B* **18** 51

[27] Zhang X L, Sui C H, Gong J, Su Z M and Qu L Y 2007 *J. Phys. Chem. C* **111** 9049

[28] Wang P, Mai Z B, Dai Z, Li Y X and Zou X Y 2009 *Biosens. Bioelectron.* **24** 3242

[29] Piela B and Wrona P K 2002 *J. Electrochem. Soc.* **149** E55

[30] Xing X and Scherson D A 1988 *Anal. Chem.* **60** 1468

[31] Mani V, Periasamy A P and Chen S M 2012 *Electrochem. Commun.* **17** 75

[32] Yang G, Yang Y, Wang Y, Yu L, Zhou D and Jia J 2012 *Electrochim. Acta* **78** 200

[33] Unnikrishnan B, Ru P L, Chen S M and Mani V 2013 *Sens. Actuators B* **177** 887

[34] Silveria G, Morais A, Villis P C M, Maroneze C M, Gushikem Y, Lucho A M S *etal* 2012 *J. Colloid Interface Sci.* **369** 302

[35] Kozub B R, Rees N and Compton R G 2010 *Sens. Actuators B* **143** 539

[36] Meng Z, Liu B and Zheng J 2011 *Microchim. Acta* **175** 251

[37] Ma Y, Song X Y, Ge X, Zhang H M, Wang G Z and Zhang Y X 2017 *J. Mater. Chem. A* **5** 4726

[38] Haldorai Y, Kimb J Y, Viliana A T, Heo N S, Huh Y S and Han Y K 2016 *Sens. Actuators B* **227** 92

[39] Kung C W, Chang T H, Chou L Y, Hupp J T, Farha O K and Ho K C 2015 *Electrochem. Commun.* **58** 51

[40] Yadav D K, Ganesan V, Sonkar P K, Gupta R and Rastogi P K 2016 *Electrochim. Acta* **200** 276

[41] Yang J H, Yang H T, Liu S H and Mao L Q 2015 *Sens. Actuators B* **220** 652